COBISS: 1.01, DOI:10.3986/ac.v51i1.10011

A SEMI-AUTOMATIC APPROACH FOR DOLINE MAPPING IN BRAZILIAN COVERED KARST: THE WAY FORWARD TO VULNERABILITY ASSESSMENT

POLAVTOMATSKI PRISTOP ZA KARTIRANJE VRTAČ NA BRAZILSKEM POKRITEM KRASU: POT DO OCENE RANLJIVOSTI

Cristiano F. FERREIRA[1,*], Yawar HUSSAIN[2] & Rogério UAGODA[3]

Abstract UDC 551.435.82:528.9(81)

Cristiano F. Ferreira, Yawar Hussain & Rogério Uagoda: A semi-automatic approach for doline mapping in Brazilian covered karst: the way forward to vulnerability assessment

Doline mapping is paramount in the vulnerability and risk assessment of the underground karst environment by identifying cave-ground connectivity points at the surface. However, manual mapping is labour-intensive, slow and subjective, especially on a large scale. Therefore, the present study adopted a GIS-based semi-automatic approach for mapping large and medium-sized depressions/dolines in the Corrente river basin in Brazil, with a particular focus on the environmentally preserved areas of river Vermelho (APANRV Portuguese abbreviation) using remote sensing (DEM and Google Earth imagery) and field-based observations. Seven typical dolines forms (e.g., cockpit with drain insertion, collapse, collapse with river capture, suffosion, solution, cover collapse, and buried) are found from extensive field surveys. As an outcome of the proposed approach, two hundred and thirty-two medium to large-sized dolines have been identified and categorised into three main groups based on the cave density and local geology G1, G2, and G3. The high density of identified dolines (164 known caves) in G1 provides reconnaissance for future speleological works in the preserved areas. Additionally, the presence of a considerable number of dolines in the adjoining areas (G2 and G3) stresses the need to revise the existing boundaries of the APANRV. Results correlate well with the dolines sites marked using field surveys and Google Earth images. This doline mapping may help researchers in the groundwater vulnerability assessment and the protection of speleological heritage preserved in the caves.

Keywords: cave-ground connectivity; preservation area; field surveying; remote sensing.

Izvleček UDK 551.435.82:528.9(81)

Cristiano F. Ferreira, Yawar Hussain in Rogério Uagoda: Polavtomatski pristop za kartiranje vrtač na brazilskem pokritem krasu: pot do ocene ranljivosti

Kartiranje vrtač je nadvse pomembno za oceno ranljivosti in tveganja podzemnega kraškega okolja, saj določa točke povezanosti med jamami in tlemi na površju. Vendar je ročno kartiranje zelo zahtevno, časovno zamudno in subjektivno, zlasti v velikih merilih. Zato je bil v tej študiji uporabljen polavtomatski pristop z uporabo orodij GIS za kartiranje velikih in srednje velikih kraških globeli/vrtač v porečju reke Corrente v Braziliji s posebnim poudarkom na okoljsko ohranjenih območjih reke Vermelho (portugalsko APANRV) z uporabo daljinskega zaznavanja (posnetki DEM in programa Google Earth) in na podlagi terenskih opazovanj. Na podlagi obsežnih terenskih raziskav je ugotovljenih sedem značilnih oblik vrtač (npr. kokpit z drenažo, udornica, udornica z zajezitvijo reke, sufozija, škavnica, udornica, nastala z udorom/rušenjem jamskega stropa, in udornice, nastale z zasutjem). Kot rezultat predlaganega pristopa je bilo opredeljenih 232 srednje velikih do velikih vrtač, ki so bile glede na gostoto vrtač in lokalno geologijo razvrščene v tri glavne skupine G1, G2 in G3. Velika gostota opredeljenih vrtač (164 znanih jam) v skupini G1 zagotavlja predhodni pregled za prihodnja speleološka dela na ohranjenih območjih. Poleg tega prisotnost velikega števila vrtač na sosednjih območjih (G2 in G3) poudarja potrebo po ponovnem pregledu zdajšnjih meja APANRV. Rezultati se dobro ujemajo z lokacijami vrtač, kartiranimi na podlagi terenskih raziskav in posnetkov programa Google Earth. To kartiranje vrtač lahko raziskovalcem pomaga pri oceni ranljivosti podzemne vode in pri zaščiti speleološke dediščine, ohranjene v jamah.

Ključne besede: povezanost med jamami in tlemi, območje varstva, terensko raziskovanje, daljinsko zaznavanje

[1] National Center for Research and Conservation of Caves – CECAV - Chico Mendes Institute for Biodiversity Conservation – ICMBio. Brasilia, 70635-800, Brazil, e-mail: cristiano.ferreira@icmbio.gov.br

[2] Georisk & Environment, Department of Geology, University of Liege, Liege, 4000, Belgium, e-mail, ORCID: yhussain@uliege.be, https://orcid.org/0000-0002-4155-6764

[3] Department of Geography, University of Brasilia, Brasilia, 70910-900, Brazil, e-mail, ORCID: rogeriouagoda@unb.br , https://orcid.org/0000-0002-9448-1313

* Corresponding author

Received/Prejeto: 22.7.2022

1. INTRODUCTION

Dolines are natural depressions present at the surface, in different sizes (diameters ranging from meters to kilometers) and shapes (circular to sub-circular) (Ford & Williams, 2007). Dolines are characteristic of karstic environments that denote the predominance of subsurface solution processes as outcomes of the interaction of slightly acidic water with soluble rocks such as carbonates. Together with the epikarst, dolines serve as a reservoir for water for the underground environment (Williams, 2008) and a direct connection between surface morphology and underground environments (fauna and speleothems) making their detailed investigation an essential step in the cave vulnerability and hazard assessment (Hussain et al., 2020a, 2020b). The identification and mapping of dolines can also be used to obtain morphometric data for karstification rate estimation and to determine the evolution of karst landscapes (Williams, 1972; Day, 1976). Doline mapping can also play a role in geological hazard assessment by helping to identify areas prone to collapse (Hofierka et al., 2018; Salles et al., 2018).

Therefore, accurate identification and mapping of dolines is a way forward leading to the vulnerability assessment of cave environments to surficial contaminants. The task is expensive and requires many resources, mainly when performed through classical photo interpretation, or field mapping, especially in large areas. To reduce such high cost, several studies have been dedicated to doline detection and mapping by applying geoprocessing tools using automated approaches on satellite images, light detection and ranging (LiDAR), digital elevation models (DEMs), or other cartographic sources (Guimarães et al., 2005; Siart et al., 2009; Carvalho Júnior et al., 2014; Wu et al., 2016; Zhu & Pierskalla, 2016; Wall et al., 2017; Cahalan & Milewski, 2018; Hofierka et al., 2018; Mihevc & Mihevc, 2021). These automatic approaches of objects (doline) identification may lead to erroneous results, especially, under limited data availability conditions. Therefore, Google Earth images and field survey-aided semi-automatic approaches are favored.

As in the case of Brazil where karst terrains are widespread, especially in the central and eastern regions of the country still, its study is in the infancy stage and requires further detailed analysis (Salles et al. 2018). The example can be taken off the Corrente river basin including APANRV, where there is still non-availability of detail databases required for the accurate identification of the dolines. An attempt had been made in the past for such identification using different geophysical techniques by Hussain et al., (2020a, 2020b). However, the scale of the study was too small to be considered for the assessment on a large scale. Therefore, there is a dire need for such mapping at a large scale using open access data.

In accordance with the needs, the present study aims to map the dolines present in the APANRV and the Corrente river basin (3,923.14 km²) in the northeastern Goiás state of Brazil. The ALOS-PALSAR and SRTM DEMs are evaluated in a semi-automated fashion together with Google Earth imagery and field surveys for a visual inspection based check on the proposed methodology. The present study's outcomes may help achieve dual objectives revising the existing boundary of the environmentally preserved areas and providing the GIS layer for the future vulnerability assessment of the underground environment.

2. MATERIAL AND METHODS

2.1 STUDY AREA DESCRIPTION

The study area covers the upper part of the Corrente river basin (Figure 1), next to the Serra Geral de Goiás. The climate of the region is tropical, with dry (April to September) and rainy (October to March) seasons presenting a precipitation index of ~1260 mm/y (Caldeira et al., 2021). There is a well-developed drainage system constituting numerous rivers (e.g., Corrente, Vermelho and Buritis) and streams (e.g., Bezerra, Piracanjuba, Rizada, Chumbada, Ventura and Extrema). Some of the watercourses become subterranean in contact with the sink, which may again emerge as resurgences or springs on the surface, promoting the formation of caves. There are also numerous depressions commonly called 'grota', which contain water in the rainy season (Hussain et al., 2020a).

The northeastern region of Goias presents stratigraphic records of the Archean, Proterozoic, Mesozoic and Cenozoic ages, most of which are Proterozoic, including the following units: Ticunzal formation, se-

quence of volcanic-sedimentary rocks of Palmeirópolis and São Domingos, the Arai group, Serra Branca, Tonalito **São** Domingos, the Paranoá group and the Bambuí group (Gaspar & Campos, 2007). The most extensive carbonate unit is the Bambuí group, which hosts the largest number of caves in Brazil. Below the sedimentary cover of the Urucuia Group, there are pelitic and carbonate rocks from the Bambuí Group (Gaspar & Campos, 2007).

The following soil classes and sediments were found: oxisoils, podzolic, cambisols, plinthsol, gleysol, sands, hydromorphic quartz, organic soils, quartz sands, alluvial soils and petroplinthic soils. The general soil classification is driven by the local geology. The soil erodibility rate is higher and related to the presence of vegetation cover (Fonseca et al., 2021). The presence of clay and claystone (between sandstone and the epikarst) act as an impermeable layer, leading to the generation of a large amount of surface runoff and sediments. The runoff may infiltrate into the karst underground at the places of geological contacts (sandstone and carbonate) and pathways to the caves (dolines/sinkholes) leading to contamination and causing a significant impact on the underground hydrological system.

The region integrates several geomorphological features: i) the escarpment; ii) the very flat upper part of the sandstone; iii) the oxisoil; iv) dolines opening in convex-concave hill-slopes under the claystone cover; v) canyons compartment formed as a result of cave collapse; and vi) the lower basing part. Four landform units were identified as canyons, deep valleys, local ridges, upland drainage, and mountain tops. Details can be found in Hussain and Uagoda (2021).

The Urucuia aquifer system has a thick layer of siliciclastic sediments and stores large groundwater volumes (Gaspar & Campos, 2007). This system covers a significant part of the area. It recharges main rivers and their tributaries (Figure 1). The presence of soluble rocks, such as the carbonates (Lagoa do Jacaré formation) in the north-central part of the area, drained by Buritis and Vermelho rivers, seems to stimulate regional denudation as compared to the southern sector. This last one presents

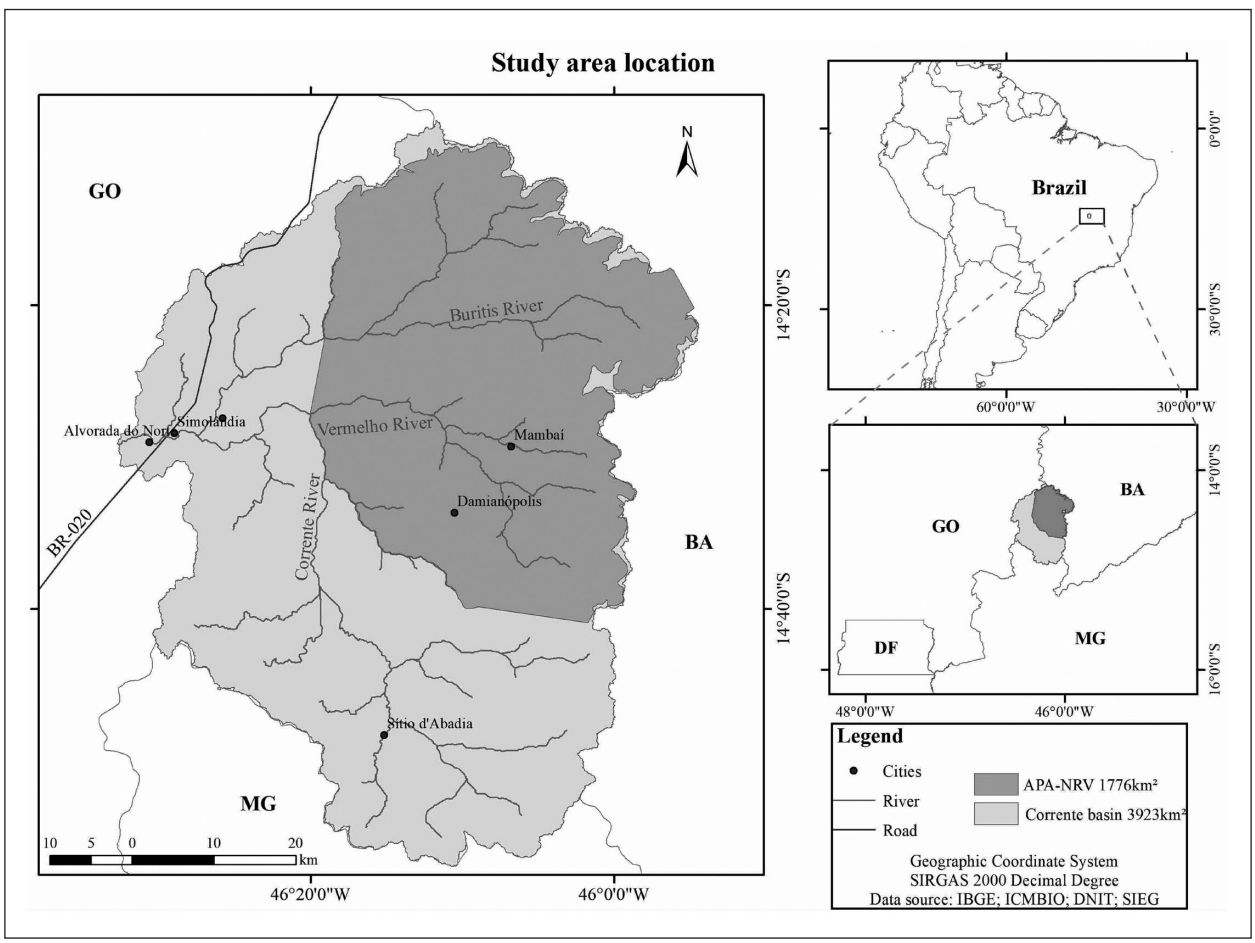

Figure 1: Location of the study area on map of Brazil, zoomed location in reference to the neighboring states and the current boundaries of APANRV along with important rivers, streams, and settlements.

lateritic surfaces that supported the relief during regressive erosion promoted by the Corrente river.

In the studied area, there are two types of cave systems have been proposed as superior/vadose (top-bottom) that collect floods from hillslopes and sediments from the nearby sandstone aquifer and deep epigene fluvial-karst (bottom-up) (Hussain & Uagoda, 2021). The Tarimba (11 km in length) is considered one of the most important (i.e., with a high level of biodiversity) and largest in the country (Hussain et al., 2020a). The caves have connectivity with the superficial environment through weak spots (the cave opening, dolines and geological contacts). In this way, land use at the surface can definitely impact the subsurface in numerous ways (i.e., water, sediments, and contaminants). So, the connectivity leads to the vulnerability of the underground environment that affect the lives of fauna and flora there. Therefore, the identification and mapping of these vulnerability-prone weak spots at the surface are crucial.

2.2 FIELD SURVEYING AND IMAGERY

For the Google Earth imagery database download, the following simple criteria of no cloud presence in the dry season and less vegetation had been adopted, which enhanced the object detection threshold many folds. After that, a doline detection criteria was adopted based on the features identification and their categorization into supportive and non-supportive. The places or polygons where there are supportive features found are considered as doline, while the opposite is true for the no doline. The places where we encountered both supportive and non-supportive features are referred to as presumed doline. The presumed and probable doline categories are, henceforth, referred to as "possible dolines". This approach is also helpful in separating karstic features from non-karstic ones as is the case with veredas (a riparian subsystem of the Cerrado biome). This image-based identification and categorization showed clear advantages over the automatic approaches where there are higher chances

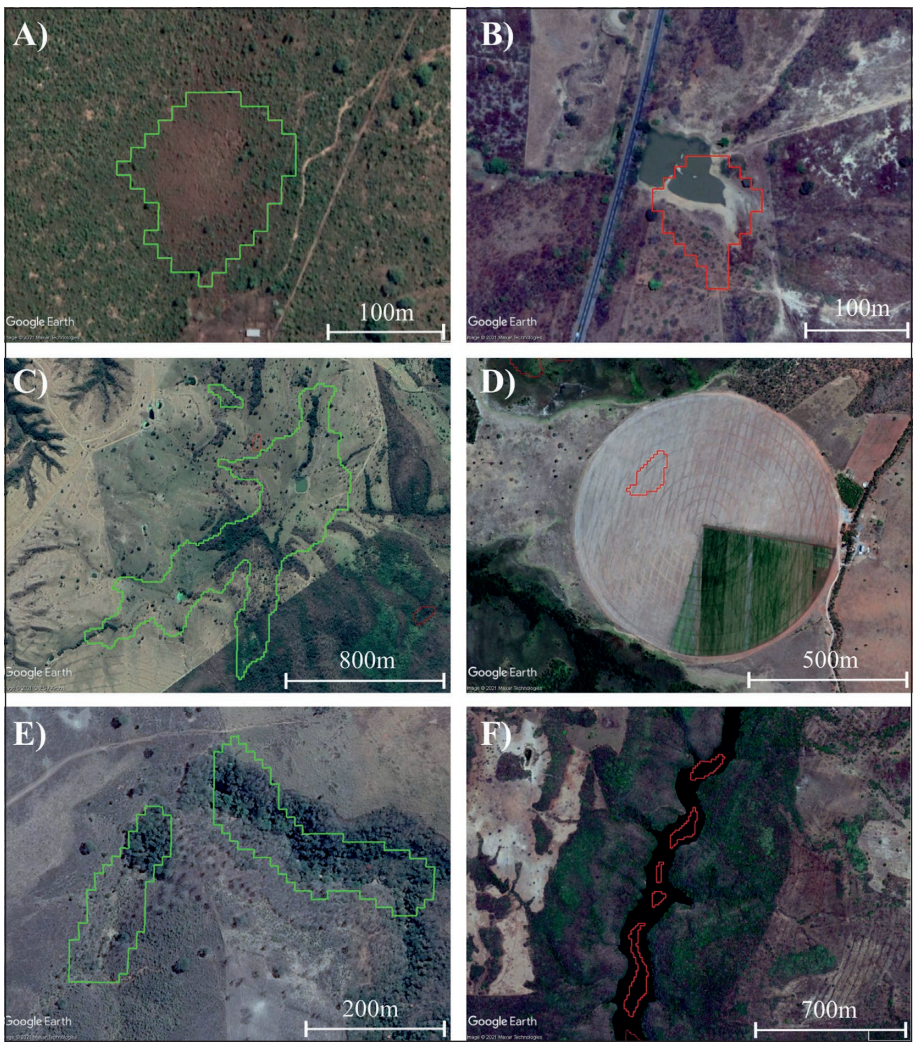

Figure 2: The visual classification results are color coded as green and red as probable and no-doline objects, respectively. A) change of vegetation in circular shape, B) depression related to road/dam, C) depression due to centripetal drainage, D) depression in anthropic areas, E) depressions with evident sinkholes and F) objects created on the canyon bottom, with open drainage. Source: Google Earth, 2020.

Probable dolines		No dolines
Centripetal drainage		Open drainage
Drainage with apparent sinkhole		Dam
Change in vegetation		Homogeneous vegetation
Soluble rock		Slightly soluble rock
Circular pattern		Atypical formats
Plateau occurrence		Grand Canyons bottom
Large and deep depression		Veredas (shallow depressions)
Cave presence		Road
Known dolines	**Presumed**	Anthropic area

Table 1: The adopted criteria for visual classification of objects into probable, possible/presumed and no dolines using Google Earth imagery.

of filtering out many features that can help in doline or depression identification. The salient features of the proposed criteria for visual inspection are presented in Table 1. Visual inspection using Google Earth imagery as a possible check on DEM-based automatic doline detection. The objects-based classification is ranked into probable dolines and no dolines. For example, the features of probable dolines are a change of vegetation in a circular shape, depression due to centripetal drainage, and depressions with evident sinkholes. The examples of the adopted inspection and marked objects on Google Earth images are presented in Figure 2.

2.3 DEM-BASED ANALYSIS

In order to check comparative performance evaluation, the DEM (12.5 m) from Advanced Land Observing Satellite Phased Arrayed type L-Band SAR (ALOS-PALSAR) and DEM (30 m) from Shuttle Radar Topography Mission (SRTM) are used (JAXA/METI, 2011; NASA, 2014).

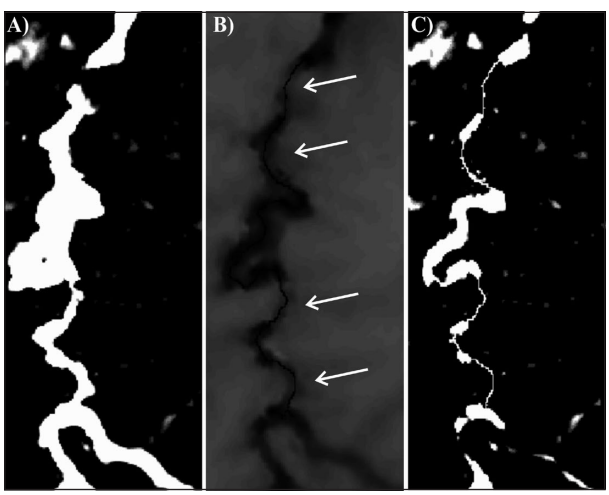

Figure 3: The grinding process of the DEM ALOS-PALSAR at narrow portions of drainage: A) large dams above 500 m wide, B) arrows point to the linear rectification performed in the original raster, and C) rectified DEM of width below 150 m.

In the end, the specific object identification capabilities of these DEMs has been enhanced using Google Earth imagery and field survey results.

After obtaining these databases (DEMs and imagery), the next step is filling of DEM-ALOS-PALSAR based on the specific conditions of the studied area. This technique identifies depressions through the arithmetic subtraction of the DEM filled from the original DEM (Bauer, 2015; Wall et al., 2017; Cahalan & Milewski, 2018; Hofierka et al., 2018). The automatic filling of DEM resulted in erroneous features especially near the watercourses and, in some cases, the formation of large "virtual dams" in narrow gorges. This has been minimized (large depressions) after applying gridding processing to the original DEM near erroneous points as recommended by Doctor and Young (2013). This narrow leveling procedure, by images, eliminates large depressions and can be applied to the erroneous points (Figure 3). This has been executed using "Serval" tool in QGIS software.

The filling is performed with the distinct altimetric filters with a Z limit value using 'Fill' tool of ArcGIS software. The fills of different values as zero (Z0), three (Z3), and ten meters (Z10) are tested. After the necessary visual inspection, we observed that Z3 limit offers a more realistic distribution of objects while Z10 showed objects only in the valley bottoms, and Z0 does not make any selection (Figure 4). Next, occurred the vectorization of the depression raster at a depth value greater than 3 m and created a column containing the area information. At this stage, the depressions below 625 m^2 (four pixels) are eliminated from the analysis based on the field experience.

The subsequent cleaning is performed based on the correlation of drainage with the objects that still remain. In the absence of hydrographic databases at the adopted scale, the drainage network has been obtained using DEM ALOS-PALSAR (Faulkner et al. 2013). A flow accumulation threshold of 500 pixels and rivers from 6th to 8th order is used (Strahler's hierarchy method) to eliminate false objects. The same aforementioned processing steps

have been repeated for DEM SRTM, except for the use of a minimum area filter because of the pixel size greater than 625 m². After visual classification of the objects from the two bases (DEMs), we classified the dolines by morphometric characteristics such as: area, perimeter, depth, and minimum altitude. The deepest point is calculated using the unprocessed DEM ALOS-PALSAR. For the dolines distribution analysis, we converted the features into centroid points which are used for the density map preparation along with known cave location maps. A complete list of doline extraction processing workflow is summarized in Figure 5.

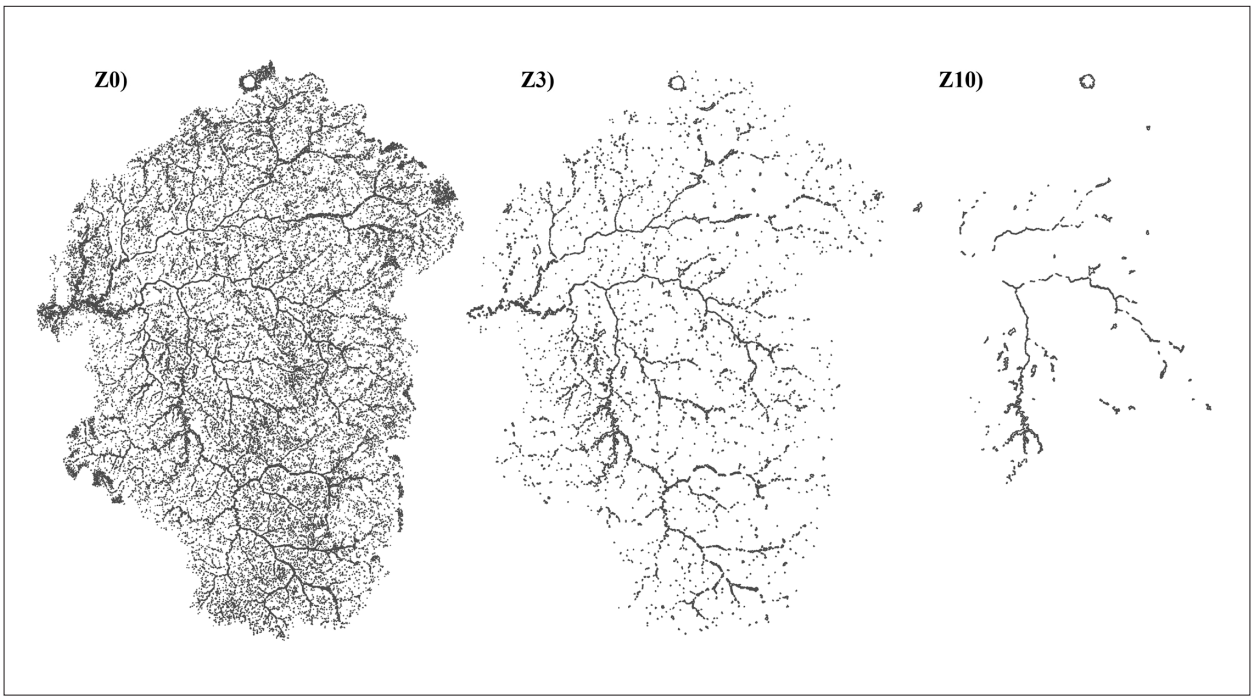

Figure 4: From left to right: Depth filters with increasing object depth from 0 m (Z0), 3 m (Z3) up to 10 m (Z10).

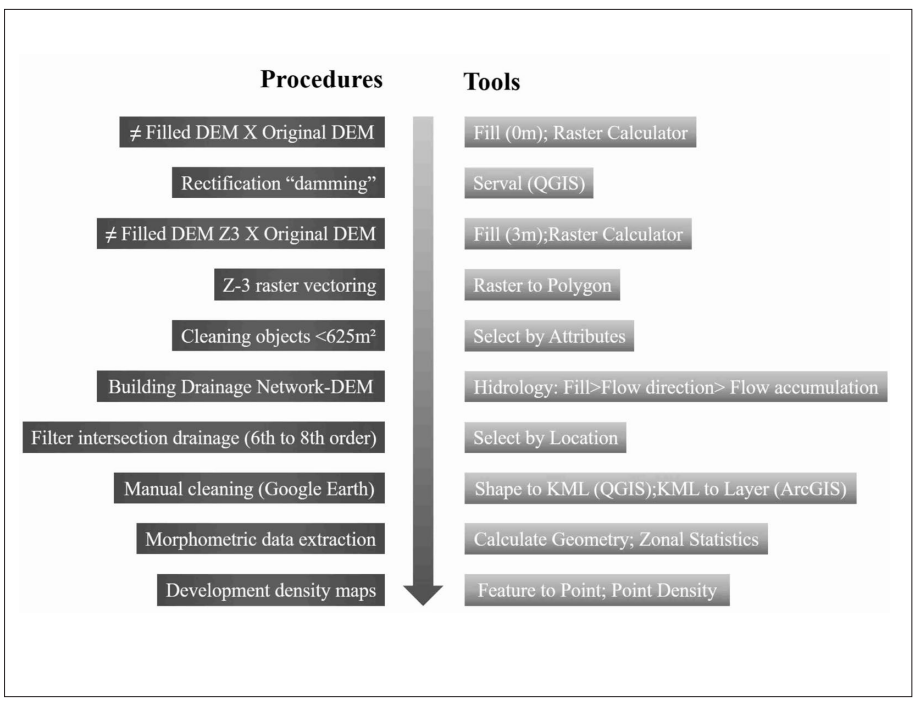

Figure 5: The processing workflow along with their execution in respective GIS tools.

3. RESULTS

3.1 DETECTION USING DEM

The comparative evaluation of DEMs resulted in identification of three more probable dolines in SRTM base than ALOS-PALSAR base. There were 11 additional objects from the SRTM base as presumed dolines. We incorporated the added elements of the landscape as dolines, rivers and hills from those bases into the final database of features as potential dolines. The quantities of classified objects into presumed, probable and no dolines in the two analyzed databases (DEMs) indicate a substantial equivalence in their detectabilities (Table 2). In spite of having a lower resolution, the SRTM base can indicate nearly the same number of objects as of ALOS-PALSAR base. However, changes in the forms of objects from these databases are observed because of variable pixel sizes. Most of the objects from SRTM went through a form change during raster to polygon conversion. There is also some over ranking in the case where larger objects are found surrounded by smaller objects. Due to these drawbacks, the ALOS-PALSAR base is used for the extraction of objects for the analysis. Despite the large data volumes and extensive manual work requirement for the inspection of numerous elements (5,706 in all), the combined analysis of these two bases ensured redundancy and greater confidence in visual classification.

Table 2: Number of objects obtained using DEMs after filtering and classification.

	ALOS	%	SRTM	%
Z0	26,410	100	25,479	100
Z3	3,377	12.79	3,430	13.46
Area < 625 m²	3,032	11.48	3,430	13.46
Drainage 6th-8th orders	2,686	10.17	3,020	11.85
Visual cleaning Google	218	0.83	213	0.84
Probable objects	99	0.37	97	0.38
Presumed objects	119	0.45	116	0.46
No dolines	2,510	9.5	2,807	11.02
Total ALOS/SRTM	232 possible dolines			

Considering the object parameters as area, perimeter, and depth (Table 3), we observe a greater extent (twice the perimeter the area) in the probable dolines as compared to the presumed ones. This discrepancy shows the difficulty in discerning smaller features using DEM, even when checked with Google Earth imagery being classified as presumed. For the minimum altitude data, the most profound points varied between 680 and 700 m. Nevertheless, it presents an occurrence at the most varied altitudes, which is compatible with covered karst being exhumed. The lowest presumed depression identified was 2,812 m², indicating that only medium to large dolines can be delineated using DEM-based analysis.

Among the identified dolines, one of much larger dimensions as 3.47 km² in the area and 20 m depth in the sandstone of the Urucuia Group, is considered as outlier and removed from the morphometric analyses (Table 3). This may possibly be created by the accommodation depression caused by underlying karst and may be referred to "sagging dolines" (Gutiérrez et al., 2008). Our methodology shows the potential of identifying large dolines (compound depressions), not considering the smaller objects inside because of the coarser scale. There are concentrations of features (dolines) in certain areas, especially of carbonates rocks. In contrast, in non-carbonate rocks (siliciclastic, pelitic, and laterites) there are large empty extensions where only a few dolines occur. The occurrence and significance of these depressions lie out of the scope of the present study and deserve future detailed investigations.

Regarding the spatial distribution, we elaborated a density map from the centroid points of all identified features and from the known cave points (Figure 6). The total number of possible dolines is 232, packed in a low overall density (0.059/km²) because of the large extent of the study area (~ 3,923.14 km²). The doline density

Table 3: Morphometric parameters of the identified depressions.

Morphometry	Probable Dolines (101)			Presumed Dolines (130)		
	Max.	Min.	Average	Max.	Min.	Average
Area (m²)	851,875	3,750	76,807	404,063	2,812	22,126
Perimeter (Km)	10.6	0.275	1.63	9.025	0.225	0.795
Depth (m)	31	3	7.89	19	3	4.55
Lowest Point (m)	956	535	683.56	959	521	702.5
Total density (nº/km²)	0.059					

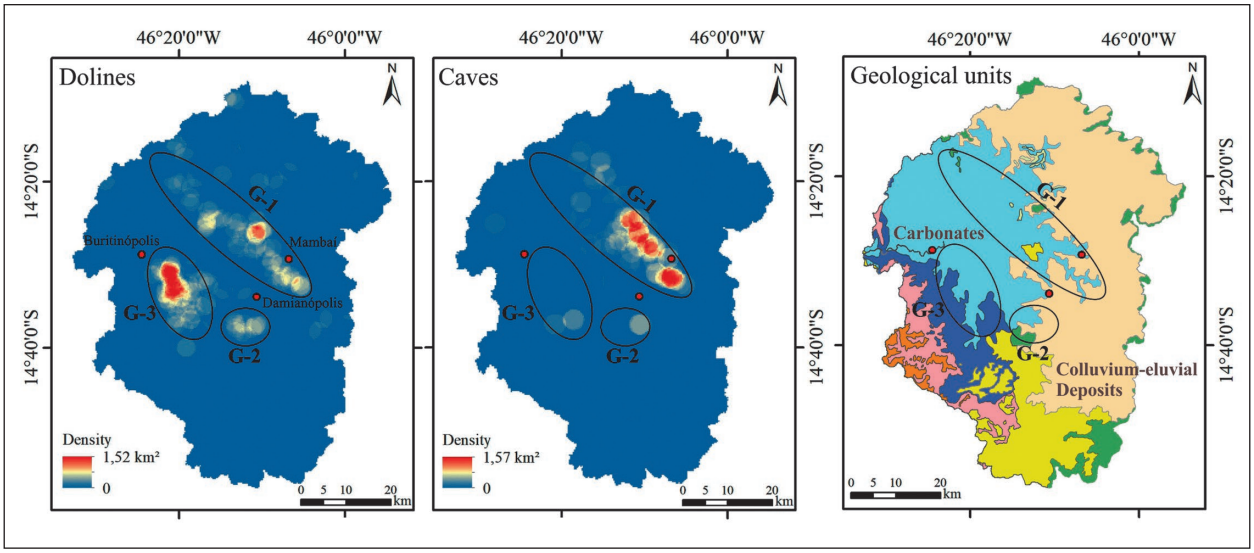

Figure 6: From left to right: dolines density, caves density and local geological maps. The groups are presented with the acronyms G-1, G-2, and G-3.

Figure 7: Typical dolines forms found in the region which may serve as the connections points between surface and underground environments: A) cockpit with drain insertion, B) collapse, C) collapse with river capture, D) suffosion; E) solution, F) cover collapse, and G) buried (Photo: C. F. Ferreira).ç

is found to correlate positively with the occurrence of carbonate rocks, such as the case with Lagoa do Jacaré formation, where 162 features are found with a density of more than double (0.155/km²) than the adjoining non-carbonated areas.

3.2 FIELD SURVEY AND IMAGERY

The local dolines, which represent the connection of surface and underground environments, are classified into various types (Figures 2 & 7). Larger composite depressions of the cockpit type, with the insertion of internal drains (channels), are quite common. Smaller collapse or suffusion features, can occur inside compound dolines and are often linked to large cave systems. Each identified typology has its own vulnerability potential and affects the underground environment accordingly.

The procedures resulted in approximately 26,000 features (Table 2). After automatic filtration, a visual analysis of only 10 to 12% of the original objects was conducted. After object inspection in DEMs as per established visual classification criteria, we obtained a total of 232 possible dolines, out of which 102 are classified as probable. The possible dolines represent less than one percent of the initial objects identified in each base (0.8%).

The dolines mapping provided an opportunity compare with the known dolines database developed as a result of successive visits in the study area, which identified smaller dolines (<1 m²), beyond the capability of automated analysis. Out of 152 field-mapped dolines in the study area, only 69 show links with 23 objects (possible) created by the semi-automatic detection of used bases, and the rest did not generate any object and are considered as trivial or pseudo features (artifacts). These 23 objects have a single or more than one dolines per object (e.g., compound dolines). The mapping performed in this work focuses more on other features because it is challenging to confirm the large dimensions of these compound dolines in the field visually. In any case, it was possible to confirm substantial dolines densification in compound dolines (Table 4). This demonstrated the effectiveness of the adopted methodology as an indicator of karst areas, where isolated minor dolines can also occur. In this case, although 83 dolines do not have associated polygons, such features are precisely present in the areas with a consequent density of large objects (Figure 8).

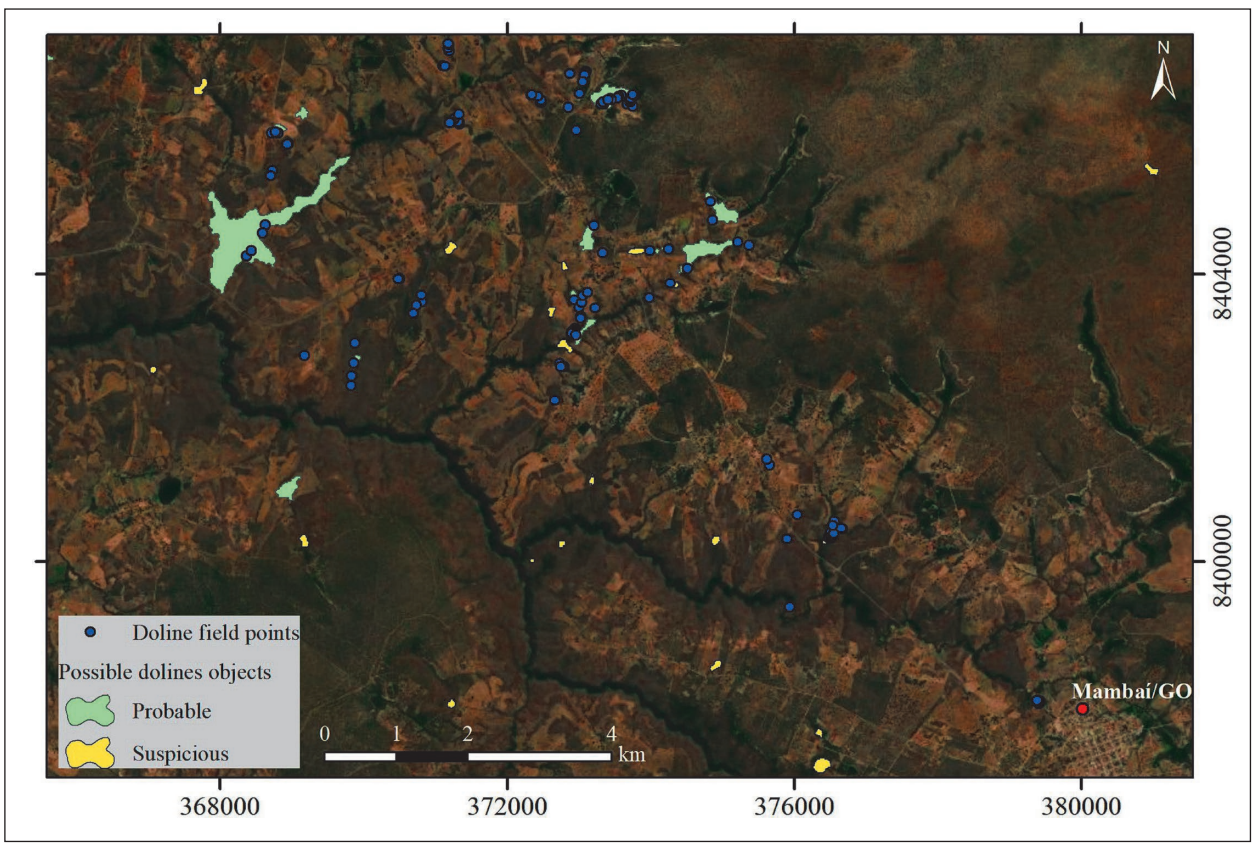

Figure 8: Doline points checked in the field, and objects considered possible dolines in Group-1. Many doline points are referred to as miniature features, which did not generate polygons at this scale (Esri et al., 2020).

Table 4: Geologywise distribution of field-mapped dolines along with their typologies.

Type/area	Group-1	Group-3	Partials
Suffosion	54	16	70
Cockpit	37	2	39
Collapse	26	1	27
Colmated	7	0	7
Solution	5	0	5
Coverage collapse	4	0	4
Totals	**133**	**19**	**152**

The predominant typologies of dolines found in the study area were the suffosion one, followed by cockpits and collapsed ones (Table 4). Colmated types, solution, and coverage collapses had appear as expected. Group-1 presented more dolines because we studied it for longer than Group-3, which rightly drew attention after the mappings performed in this research. Both areas and all other objects generated in this work still require further confirmation. The results indicate areas prone to depression occurrence as a reconnaissance for further field activities in order to refine the mapping of undetected dolines and caves.

4. DISCUSSION

The geologywise distribution of these possible dolines is mainly characterized in three groups: i) the first, a NW-SE trend near the sandstone-limestone contact at the north of Mambaí (Group-1); ii) the second of lesser prominence, south of Damianópolis (Group-2); and iii) the third and most dense, southeast of Buritinópolis (Figure 6). Compared with the cave density map, we see an evident density convergence in these features with Group-1 dolines in the previous map. There is also a relationship between caves and Group-2 dolines. Group-3 has nearly no cave presence.

It is essential to highlight that the doline density map presents the result of an investigation based on remote sensing without field confirmation of all features. Thus, it may explain the occurrence of scattered sectors on the map with a substantial density, not included in any group mentioned, which may or may not contain dolines. On the other hand, the density in Group-3 and the convergence with the cave density of Groups 1 and 2 allow us to assume a greater possibility of features in such areas. The three identified groups converge at a greater or lesser degree with the occurrence of carbonates of the Lagoa do Jacaré formation as observed by overlapping the features with the geological map (Figure 6). Scattered occurrences are associated with alluvial-colluvial clastic deposits from the Serra Geral de Goiás erosion. The carbonate occurrence under the clastic sediments, especially at the intersection of G-1 and G-2, indicates a process of exhumation in the karst.

No cave corresponding to group-3 may attribute to the fact that the area has not yet been the target of systematic speleological prospecting. Hence, we carried out a more accurate interpretative analysis by Google Earth images at the basin scale compared to the overflow level as documented in the literature (Telbisz et al. 2009; Bauer, 2015). Results show a polygonal typology for the local karst (Williams, 1972), something unexpected if considered the recurrent pattern of adjacent karst areas, with

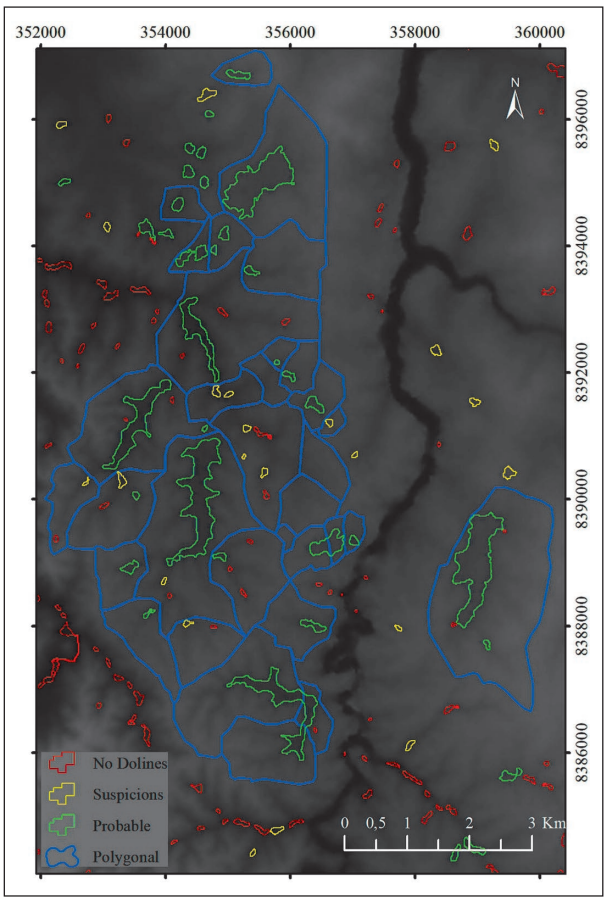

Figure 9: Polygonal karst patterns (in blue), objects in green (probable dolines), yellow (presumed dolines), and red (no dolines) were identified by the automatic approach. Source: DEM ALOS-PALSAR (JAXA/METI, 2011).

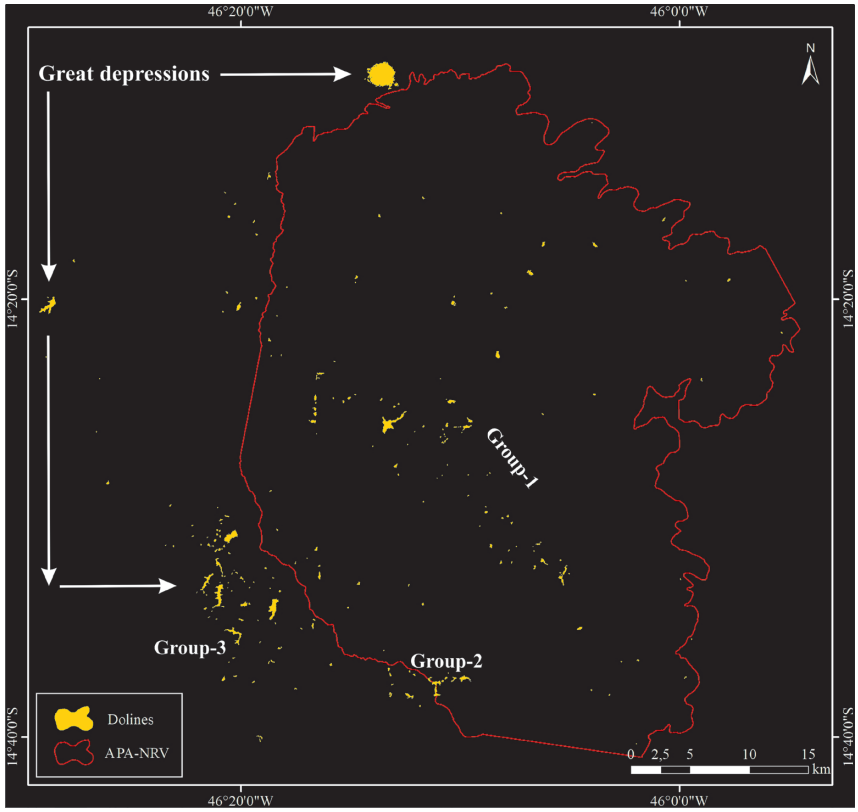

Figure 10: Spatial distribution of the possible dolines in the Corrente river basin and the APANRV borders.

isolated dolines in the landscape (Figure 9). Visual inspection also allowed the identification of other dolines, not pointed out in the automated process, and the subdivision of depressions during the filtration process (Z3). The semi-automated methodology could be applied for the initial detection of dolines but requires further visual refinement for checking and delimitation, as recommended by Hiruma and Ferrari (2014).

Results obtained within in the boundaries of the APANRV show that large karst structures occur outside the current limits of the preservation area (Group-3) and in adjacent areas (Group-2), highlighting the need for quick actions (Figure 10). Along with the isolated features, the polygonal or sagging depressions are also found outside the limits of the APANRV. These features indicate high capacities of surface water conduction to the underground environment, which increases the exposure of these areas to contamination of the karst aquifers.

Thus, in order to fulfill the local speleological conversion objectives in the APANRV, it is necessary to expand the current boundaries of the preserved area to encompass these large karst structures in the adjoining areas. The location of the large, medium, and small dolines are areas of water recharge for karst systems. The preservation of the underground environment requires proper land use managerial plans, which prohibit the installation of large projects for agriculture, mining, highways, and other related incompatible activities.

If we consider the lack of other detailed databases and the existing doline maps, it is fair to affirm that the procedures we adopted have filled the existing knowledge gap regarding the identification of karst features. This new information can be added to the future planning of the APANRV through the reconnaissance of speleological prospection and mapping of small-scale dolines.

5. CONCLUSIONS AND RECOMMENDATION

In areas of substantial territorial extension, doline mapping is a complex task that becomes even harder using manual and non-automated techniques. The integrated use of DEM, along with high-resolution images represents an additional source of information that can be explored with geo-technological resources for doline

mapping and even beyond. We used the DEM ALOS-PALSAR and SRTM in this work, applying series of automated procedures aimed at identification of medium to large karst depressions. The results show that, although the digital models do not present resolutions compatible with the detection of small dolines, they are essential for identifying karstified areas, in which large and medium depressions occur, but also small features. The analysis of two models in parallel ensured redundancy, complementarity, and greater confidence in the classification of objects. Surprisingly, the SRTM base, with lower spatial resolution, presented results equivalent to ALOS-PALSAR, demonstrated its versatility.

Thus, from this research, we identified dominant density areas for possible dolines, the presence of isolated dominant features, and structures of high hydrological significance, such as polygonal karst zones. Such data will be available for the future Planning Phase of the APANRV, directing detailed confirmations on the field. The results also show areas of high speleological potential, indicating the methodology is applicable to regions under investigation for cave occurrence as caves and dolines have a significant evolutionary and environmental role. The observation of regional karstification processes and indication points of higher water concentration and aquifers vulnerability can be evaluated. For mapping the presence of features of different dimensions and forms, high resolution drone-based photogrammetry and further detailed field surveying are recommended.

The doline map can be considered a raster for the cave underground vulnerability assessment using a suitable index-based karst vulnerability models. Around the identified dolines and caves, buffer zones of certain diameter based on the field survey could be chosen. The afterword rating system could be signed to each buffer zone based on its proximity to the vulnerability-prone features such as a river, agricultural forms, industry, gas pumps etc.

REFERENCES

Bauer, C., 2015: Geomorphology Analysis of dolines using multiple methods applied to airborne laser scanning data.- Geomorphology, 250, 78–88. DOI: 10.1016/j.geomorph.2015.08.015

Cahalan, M.D. & A.M. Millewski, 2018: Sinkhole formation mechanisms and geostatistical-based prediction analysis in a mantled karst terrain.- Catena, 165, 333–344. DOI: 10.1016/j.catena.2018.02.010

Caldeira, D., Uagoda, R., Nogueira, A.M., Garnier, J., Sawakuchi, A.O. & Y. Hussain, 2021: Late Quaternary episodes of clastic sediment deposition in the Tarimba Cave, Central Brazil. *Quaternary International*, *580*, 22–37. DOI: 10.1016/j.quaint.2021.01.012

Carvalho Júnior, O.A., Guimarães, R.F., Montgomery, D.R., Gillespie, A.R., Gomes, R.A.T., Martins, E.S. & N.C. Silva, 2014: Karst depression detection using ASTER, ALOS/PRISM and SRTM-derived digital elevation models in the Bambuí Group, Brazil.- Remote Sensing, 6, 330–351. DOI: 10.3390/rs6010330

Day, M., 1976: The morphology and hydrology of some Jamaican karst depressions. Earth Surface Processes, 1, 111–129. DOI: 10.1002/esp.3290010203

Doctor, D.H. & J.A. Young, 2013: An evaluation of automated GIS tools for delineating karst sinkholes and closed depressions from 1-meter LiDAR-derived digital elevation data.- In: Land, L., Doctor, D.H. & J.B. Stephenson (Eds.) *Proceedings of the 13th Multidisciplinary Conference on Sinkholes and the Engineering and Environmental Impacts of Karst*, 13th, 2013, New Mexico, National Cave and Karst Research Institute, 449–458. DOI: 10.5038/9780979542275.1156

Esri, Maxar, Geo Eye, Earthstar Geographics, CNES/Airbus DS, USDA, USGS, AeroGrid, IGN, & GIS User Community, 2020. World Imagery. Available from: https://www.arcgis.com/home/item.html?id=10df2279f9684e4a9f6a7f08febac2a9 [Accessed 6th January 2020].

Faulkner, M.G.S., Stafford, K.W. & A.W. Bryant, 2013: Delineation and classification of karst depressions Using LIDAR: Fort Hood Military Installation, Texas.- In: Land, L., Doctor, D.H. & J.B. Stephenson (Eds.) *Proceedings of the 13th Multidisciplinary Conference on Sinkholes and the Engineering and Environmental Impacts of Karst*, 13th, 2013, New Mexico, National Cave and Karst Research Institute, 459–467. DOI: 10.5038/9780979542275.1157

Fonseca, M.R.S., Uagoda, R. & H.M.L. Chaves, 2021: Rates, factors, and tolerances of water erosion in the Cerrado biome (Brazil): A meta-analysis of runoff plot data. *Earth Surface Processes and Landforms*, *47*(2), 582–595. DOI: 10.1002/esp.5273

Ford, D.C. & P.W. Williams, 2007: Karst Hydrogeology and Geomorphology.- Wiley, pp. 562, Chichester.

Gaspar, M.T.P. & J.E.G. Campos, 2007: O sistema

aqüífero Urucuia.- Revista Brasileira de Geociências, 37, 4, 1068–1078. DOI: 10.25249/0375-7536.200737S4216226

Google Earth, 2020: Google Earth Pro, version 7.3.4.8642 (64-bit). Available from: http://www.google.com/earth/index.html [Accessed 6th January 2020].

Guimarães, R.F., Carvalho Júnior, O.A., Martins, E.S., Carvalho, A.P.F. & R.A.T. Gomes, 2005: Detection of karst depression by aster image in the Bambui Group, Brazil.- SPIE, 5983, 328–339. DOI: 10.1117/12.627741

Gutiérrez, F., Guerrero, J. & P. Lucha, 2008: A genetic classification of sinkholes illustrated from evaporite paleokarst exposures in Spain.- Environmental Geology, 53, 993–1006. DOI: 10.1007/s00254-007-0727-5

Hiruma, S.T. & J.A. Ferrari, 2014: Análise comparativa da extração automatizada de dolinas a partir de modelos digitais de terreno.- Revista do Instituto Geológico, 34, 2, 1–11. DOI: 10.5935/0100-929X.20140006

Hofierka, J., Gallay, M., Bandura, P. & J. *Šašak*, 2018: Identification of karst sinkholes in a forested karst landscape using airborne laser scanning data and water flow analysis.- Geomorphology, 308, 265–277. DOI: 10.1016/j.geomorph.2018.02.004

Hussain, Y., & R. Uagoda, 2021: GIS-based relief compartment mapping of fluvio-karst landscape in central Brazilian highlands.- International Journal of Economic and Environmental Geology. DOI: 10.1002/essoar.10503441.2

Hussain, Y., Uagoda, R., Borges, W., Prado, R.L., Hamza, O., Cárdenas-Soto, M., Havenith, H-B. & J. Dou, 2020a: Detection of cover collapse doline and other Epikarst features by multiple geophysical techniques, case study of Tarimba cave, Brazil.- Water, 12(10), 2835. DOI: 10.3390/w12102835

Hussain Y, Uagoda R, Borges W, Nunes J, Hamza O, Condori C, Aslam K, Dou J, Cárdenas-Soto M. 2020b: The Potential Use of Geophysical Methods to Identify Cavities, Sinkholes and Pathways for Water Infiltration. Water; 12(8):2289. https://doi.org/10.3390/w12082289

JAXA/METI, 2011: ALOS PALSAR ALPSRP267816890, ASF DAAC. Available from: https://asf.alaska.edu. DOI 10.5067/Z97HFCNKR6VA [Accessed 11th July 2018].

Mihevc, A. & R. Mihevc, 2021: Morphological characteristics and distribution of dolines in Slovenia, a study of a lidar-based doline map of Slovenia.- Acta Carsologica 50/1, 11–36. DOI: 10.3986/ac.v50i1.9462

NASA, 2014 SRTM 1 Arc-Second Global, SRTM-1S15W047V3, SRTM1S15W046V3. Available from: https://earthexplorer.usgs.gov/ [Accessed 22nd September 2018].

Salles, L.Q., Galvão, P., Leal, L.R.B., Pereira, R.G.F.A., Purificação, C.G.C. & F.V. Laureano, 2018: Evaluation of susceptibility for terrain collapse and subsidence in karst areas, municipality of Iraquara, Chapada Diamantina (BA), Brazil.- Environmental Earth Sciences, 77, 16, 593. DOI: 10.1007/s12665-018-7769-8

Siart, C., Bubenzer, O. & B. Eitel, 2009: Combining digital elevation data (SRTM/ASTER), high resolution satellite imagery (quickbird) and GIS for geomorphological mapping: A multi-component case study on Mediterranean karst in Central Crete.- Geomorphology, 112, 1-2, 106–121. DOI: 10.1016/j.geomorph.2009.05.010

Telbisz, T., Dragušica, H. & B. Nagy, 2009: Doline Morphometric analysis and karst morphology of Biokovo Mt (Croatia) based on field observations and digital terrain analysis.- Hrvatski geografski glasnik, 71, 2, 5–22. DOI: 10.21861/hgg.2009.71.02.01

Wall, J., Bohnenstiehl, D.R., Wegmann, K.W. & N.S. Levine, 2017: Morphometric comparisons between automated and manual karst depression inventories in Apalachicola National Forest, Florida, and Mammoth Cave National Park, Kentucky, USA.- Natural Hazards, 85, 2, 729–749. DOI: 10.1007/s11069-016-2600-x

Williams, P.W, 2008: The role of the epikarst in karst and cave hydrogeology: a review.- International Journal of Speleology, 37, 1, 1–10. DOI: 10.5038/1827-806X.37.1.1

Williams, P.W., 1972: Morphometric analysis of polygonal karst in New Guinea.- Geological Society of America Bulletin, 83, 3, 761–796. DOI: 10.1130/0016-7606(1972)83[761:MAOPKI]2.0.CO;2

Wu, Q., Deng, C. & Z. Chen, 2016: Automated delineation of karst sinkholes from LiDAR-derived digital elevation models.- Geomorphology, 266, 1–10. DOI: 10.1016/j.geomorph.2016.05.006

Zhu, J. & W.P. Pierskalla, 2016: Applying a weighted random forests method to extract karst sinkholes from LiDAR data.- Journal of Hydrology, 533, 343–352. DOI: 10.1016/j.jhydrol.2015.12.012